Applied Mathematics Letters 89 (2019) 28–34

Contents lists available at ScienceDirect

Applied Mathematics Letters

www.elsevier.com/locate/aml

Non-singular Green's functions for the unbounded Poisson equation in one, two and three dimensions

Mads Mølholm Hejlesen [a], Grégoire Winckelmans [b], Jens Honoré Walther [a,c,*]

[a] *Department of Mechanical Engineering, Technical University of Denmark, Kgs. Lyngby, Denmark*
[b] *Institute of Mechanics, Materials and Civil Engineering, Université catholique de Louvain, Louvain-la-Neuve, Belgium*
[c] *Computational Science and Engineering Laboratory, ETH Zürich, Zürich, Switzerland*

ARTICLE INFO

Article history:
Received 23 August 2018
Received in revised form 18 September 2018
Accepted 18 September 2018
Available online xxxx

Keywords:
Partial differential equations
Poisson equation
Green's function
Unbounded domain

ABSTRACT

In this paper, we derive the non-singular Green's functions for the unbounded Poisson equation in one, two and three dimensions using a spectral cut-off function approach to impose a minimum length scale in the homogeneous solution. The resulting non-singular Green's functions are relevant to applications which are restricted to a minimum resolved length scale (e.g. a mesh size h) and thus cannot handle the singular Green's function of the continuous Poisson equation. We furthermore derive the gradient vector of the non-singular Green's function, as this is useful in applications where the Poisson equation represents potential functions of a vector field.

1. Introduction

Green's functions are the preferred methods for solving linear differential equations in an unbounded domain, i.e. with free-space boundary conditions. The Green's function represents a homogeneous solution which is derived analytically, and then used to obtain the particular solution by a convolution with the right-hand-side field of the Poisson equation.

The analytical Green's function of a continuous smooth field is singular at its origin. Applied in discretized numerical calculations, the singularity of the Green's function evidently causes a number of difficulties. In order to amend this, smoothing regularization techniques have been applied (e.g. [1–3]) which introduce a continuous and smooth field distribution around the discrete points and thus avoid the singularity of the Green's function. However, most regularization methods that have been applied are based on functions that only conserve a finite number of field moments, and are thus only accurate up to a finite order of convergence rate.

* Correspondence to: Department of Mechanical Engineering, Technical University of Denmark, Building 403, DK-2800 kgs. Lyngby, Denmark.
E-mail address: jhw@mek.dtu.dk (J.H. Walther).

https://doi.org/10.1016/j.aml.2018.09.012
0893-9659/

Vico et al. [4] derived non-singular Fourier transforms of the Green's function in two and three dimensions by imposing an isotropic maximum length scale of the integrated domain in real space. This method was shown to provide a spectral accuracy when the computational domain was sufficiently extended in all directions to provide a sufficient spectral resolution when evaluating the Green's function in Fourier space. However, as the Green's function is isotropic the imposed maximum length scale dictates the spectral resolution criteria, and thus the length of the integrated domain, for all directions. This makes the method of Vico et al. [4] potentially inefficient for elongated domains, as the imposed length scale must be proportional to the maximum length of the domain to insure that the integration includes the full domain.

In this work we impose a minimum length scale in the real space, analogous to a discretization length, in order to obtain a non-singular expression to the real space Green's function. This is achieved using a spectral cut-off function to avoid the aforementioned singularity in the real space representation. By using a spectral cut-off function, we impose a minimum length scale, allowing us to derive the Green's function analytically. As no explicit smoothing function is applied, the obtained non-singular Green's function gives an optimal accuracy when used in numerical calculations, as it is only subject to quadrature errors, converging in a rate proportional to the smoothness of the right-hand-side field.

As with the method of Vico et al. [4] the presented method also imposes an isotropic length scale for all directions, albeit here as a minimum length scale of the solution. Consequently, if the discretization is non-isotropic the proposed method will provide a solution, in all directions, which is limited to the minimum length scale of the lowest resolved direction.

The gradient vector of the non-singular Green's function is also derived. This function is useful in applications where the Poisson equation represents a vector or scalar potential function of a vector field as it enables a direct solution of the vector field.

The proposed non-singular Green's functions may be used directly in efficient computational methods such as the fast multipole method [5,6] or the mesh based FFT solver [7]. The mesh based Poisson solver was recently shown capable of obtaining a high order convergence rate by using regularized Green's functions [8–10]. The mesh based solver was extended to handle mixed unbounded and periodic boundary conditions by Chatelain and Koumoutsakos [11] and for high order accuracy in Spietz et al. [12]. Here the periodic Green's function solution is combined with that of an unbounded solution of reduced dimensionality.

Using the non-singular Green's functions presented here in the mesh based Poisson solver effectively results in a solution of spectral accuracy. The reader is referred to the open source software [13] for a numerical implementation of this.

2. Methodology

The Poisson equation in an unbounded domain is formally stated as:

$$\boldsymbol{\nabla}^2 A(\boldsymbol{x}) = -B(\boldsymbol{x}) \qquad \text{where} \qquad A(\boldsymbol{x}) \to 0 \quad \text{for} \quad |\boldsymbol{x}| \to \infty \tag{1}$$

Here $B(\boldsymbol{x})$ is a known bounded field and $A(\boldsymbol{x})$ is the desired solution field. In many applications such as astrophysics, electrodynamics and vortex dynamics, the vector field to be solved $\boldsymbol{v}(\boldsymbol{x})$ is described by potential functions using the Helmholtz decomposition:

$$\boldsymbol{v}(\boldsymbol{x}) = \boldsymbol{\nabla} \times \boldsymbol{\psi}(\boldsymbol{x}) - \boldsymbol{\nabla}\phi(\boldsymbol{x}) \qquad \text{where} \qquad \boldsymbol{\nabla} \cdot \boldsymbol{\psi}(\boldsymbol{x}) = 0 \tag{2}$$

The fundamental operations describing the conservation of the flux and circulation of the vector field $\boldsymbol{v}$ is the divergence $\vartheta(\boldsymbol{x}) = \boldsymbol{\nabla} \cdot \boldsymbol{v}(\boldsymbol{x})$ and the curl $\boldsymbol{\omega}(\boldsymbol{x}) = \boldsymbol{\nabla} \times \boldsymbol{v}(\boldsymbol{x})$, respectively. From Eq. (2) it follows that these may be expressed by the potential functions as:

$$\vartheta(\boldsymbol{x}) = -\boldsymbol{\nabla}^2\phi(\boldsymbol{x}) \qquad \text{and} \qquad \boldsymbol{\omega}(\boldsymbol{x}) = -\boldsymbol{\nabla}^2\boldsymbol{\psi}(\boldsymbol{x}) \tag{3}$$

Both potentials may thus be obtained by solving a Poisson equation. By utilizing the linearity of the Poisson equation, and considering the equations by their Fourier transform, we obtain the algebraic equations:

$$\begin{array}{l} -k^2\widehat{\phi}(\boldsymbol{k}) = -\widehat{\vartheta}(\boldsymbol{k}) \\ -k^2\widehat{\boldsymbol{\psi}}(\boldsymbol{k}) = -\widehat{\boldsymbol{\omega}}(\boldsymbol{k}) \end{array} \quad \Rightarrow \quad \begin{array}{l} \widehat{\phi}(\boldsymbol{k}) = \widehat{G}(\boldsymbol{k})\,\widehat{\vartheta}(\boldsymbol{k}) \\ \widehat{\boldsymbol{\psi}}(\boldsymbol{k}) = \widehat{G}(\boldsymbol{k})\,\widehat{\boldsymbol{\omega}}(\boldsymbol{k}) \end{array} \quad \text{where} \quad \widehat{G}(\boldsymbol{k}) = \frac{1}{k^2} \tag{4}$$

Here $\widehat{\cdot}$ denotes a Fourier transformed variable, ι the imaginary unit, $\boldsymbol{k}$ is the angular wave-number of the Fourier space, and $k = |\boldsymbol{k}|$ its modulus. $\widehat{G}(\boldsymbol{k})$ is the Green's function in Fourier space which represents the homogeneous solution to the Poisson equation. We may furthermore obtain the vector field of Eq. (2) directly by incorporating the gradient operator into the Green's function as $\boldsymbol{K}(\boldsymbol{x}) = \boldsymbol{\nabla} G(\boldsymbol{x})$ after which:

$$\begin{array}{l} -k^2\,\widehat{\boldsymbol{v}}_\vartheta(\boldsymbol{k}) = -\iota\boldsymbol{k}\,\widehat{\vartheta}(\boldsymbol{k}) \\ -k^2\,\widehat{\boldsymbol{v}}_\omega(\boldsymbol{k}) = -\iota\boldsymbol{k}\times\widehat{\boldsymbol{\omega}}(\boldsymbol{k}) \end{array} \quad \Rightarrow \quad \begin{array}{l} \widehat{\boldsymbol{v}}_\vartheta(\boldsymbol{k}) = \widehat{\boldsymbol{K}}(\boldsymbol{k})\,\widehat{\vartheta}(\boldsymbol{k}) \\ \widehat{\boldsymbol{v}}_\omega(\boldsymbol{k}) = \widehat{\boldsymbol{K}}(\boldsymbol{k})\times\widehat{\boldsymbol{\omega}}(\boldsymbol{k}) \end{array} \quad \text{where} \quad \widehat{\boldsymbol{K}}(\boldsymbol{k}) = \frac{\iota\boldsymbol{k}}{k^2} \tag{5}$$

As the Green's function in Fourier space (Eq. (4)) is in fact unbounded, an infinite domain in the Fourier space is needed in order to obtain the correct solution. However, for a discrete approximation, such as is used in numerical simulations, the discretization of the domain in the physical space results in a bounded domain in the Fourier space, represented by the set of wave-numbers $k_i = \{-k_s/2, \ldots, k_s/2\}$. Here $k_s = 2\pi/h$ is the angular sampling wave-number corresponding to the discretization length h and $k_s/2$ is the highest resolved angular wave-number due to the Nyquist–Shannon sampling theorem. The exact Green's function of Eq. (4) thus cannot not be represented in a discretized space, and using it will introduce errors in the calculation resulting in a limited convergence rate of $\mathcal{O}(h^2)$ [14].

In order to amend this and derive a Green's function which is bounded by a maximum wavenumber, we regularize the Green's function using a radial cut-off function in Fourier space:

$$\widehat{\zeta}(k) = \begin{cases} 1 & \text{for} \quad 0 < k \leq \dfrac{k_s}{2} \\ 0 & \text{for} \quad k > \dfrac{k_s}{2} \end{cases} \tag{6}$$

This leads to a regularized Green's function and a corresponding homogeneous equation of:

$$\widehat{G}(k) = \frac{\widehat{\zeta}(k)}{k^2} \qquad \Rightarrow \qquad \boldsymbol{\nabla}^2 G(r) = -\zeta(r) \tag{7}$$

Using the radial cut-off function of Eq. (6), it is seen that the Green's function of the non-regularized equation (Eq. (4)) is unchanged in the range of wave-numbers $0 < k \leq k_s/2$.

3. Results

By utilizing the radial symmetry of the Green's function, the regularization function in real space $\zeta(\rho)$ may be obtained by considering the unbounded Fourier transform in d-dimensional spherical/polar coordinates which is given by:

$$\widehat{\zeta}(s) = (2\pi\sigma^2)^{\frac{d}{2}} \int_0^\infty \zeta(\rho)\, \frac{J_{\frac{d}{2}-1}(s\rho)}{(s\rho)^{\frac{d}{2}-1}} \rho^{d-1}\, d\rho \tag{8}$$

where J_ν denotes the Bessel function of the first kind and of order ν. Using an integral identity of the Bessel functions [15], we may satisfy Eq. (6) by using the cut-off function:

$$\widehat{\zeta}(s) = \int_0^\infty \frac{J_{\frac{d}{2}}(\rho) J_{\frac{d}{2}-1}(s\rho)}{s^{\frac{d}{2}-1}}\, d\rho = \begin{cases} 1 & \text{for} \quad 0 < s < 1 \\ 1/2 & \text{for} \quad s = 1 \\ 0 & \text{for} \quad 1 < s \end{cases} \tag{9}$$

Here we have shifted to normalized coordinates $s = \sigma k$ and $\rho = r/\sigma$ where σ is determined by fulfilling $s = 1$ for $k = k_s/2$:

$$\sigma \frac{k_s}{2} = \sigma \frac{\pi}{h} = 1 \qquad \Rightarrow \qquad \sigma = \frac{h}{\pi} \qquad \Rightarrow \qquad s = \frac{hk}{\pi} \quad \text{and} \quad \rho = \frac{\pi r}{h} \tag{10}$$

Here h is an isotropic minimum length scale. In case of a non-isotropic discretization, h must be chosen as the largest discretization length in order to ensure that the Green's function is sufficiently resolved in all directions. This however, comes at the cost of low-pass filtering the higher resolved directions and hence an isotropic discretization is preferred for this method.

Considering Eqs. (8) and (9), we find that the regularization function in real space is given by:

$$\zeta(\rho) = \frac{J_{\frac{d}{2}}(\rho)}{(2\pi\sigma^2\rho)^{\frac{d}{2}}} \tag{11}$$

For the case of $d = 2$ this is identical to that presented in Refs. [1,3].

We may now obtain the corresponding real space Green's function by radial integration of the homogeneous equation (Eq. (7)) in the unbounded real space. For the one-dimensional case ($d = 1$), we obtain:

$$G(\rho) = -\frac{\sigma}{\pi}\left(\mathrm{Si}(\rho)\rho + \cos(\rho)\right) + C_1 \qquad \text{for} \quad d = 1 \tag{12}$$

Here $\mathrm{Si}(\rho) = \int_0^\rho \frac{\sin(q)}{q}\, dq$ is the sine integral function and C_1 is an arbitrary integration constant, which we may use to define a reference value. In this work we determine C_1 such that we obtain an asymptotic behavior towards the non-regularized Greens function for large ρ whatever the value of σ:

$$C_1 = \frac{1}{2}L \qquad \Rightarrow \qquad G(\rho) \to -\frac{1}{2}(r - L) \qquad \text{for} \quad \rho \to \infty \tag{13}$$

Here L is a chosen global reference length of arbitrary value.

The gradient vector of the Green's function, which may be used to combine the gradient operator directly in Eq. (5), is given by:

$$K(\rho) = -\frac{\mathrm{Si}(\rho)}{\pi} \qquad \text{for} \quad d = 1 \tag{14}$$

Similarly, for the two-dimensional case ($d = 2$) the radial integration yields the real space Green's function:

$$G(\rho) = -\frac{1}{2\pi}\mathrm{Ji}_0(\rho) + C_2 \qquad \text{for} \quad d = 2 \tag{15}$$

where $\mathrm{Ji}_0(\rho) = \int_0^\rho \frac{1 - J_0(q)}{q}\, dq$ is the Bessel integral function which for a numerical implementation may be approximated efficiently e.g. by Chebyshev polynomials cf. [16]. C_2 is an arbitrary integration constant, which we may use to define a reference value. Again, we determine the integration constant C_2 such that we obtain an asymptotic behavior towards the singular Greens function for large ρ whatever the value of σ:

$$C_2 = -\frac{1}{2\pi}\ln\left(\frac{2\sigma}{L}\right) + \gamma \qquad \Rightarrow \qquad G(\rho) \to -\frac{1}{2\pi}\ln\left(\frac{r}{L}\right) \qquad \text{for} \quad \rho \to \infty \tag{16}$$

Here L is a chosen global reference length.

The gradient vector of the Green's function, which may be used to calculate the vector field directly in Eq. (5), is given by:

$$\boldsymbol{K}(\rho) = -K(\rho)\boldsymbol{e}_r \quad \text{with} \quad K(\rho) = -\frac{1}{\sigma}\frac{dG(\rho)}{d\rho} = \frac{1}{2\pi\sigma}\frac{1 - J_0(\rho)}{\rho} \qquad \text{for} \quad d = 2 \tag{17}$$

Here $K(\rho) \geq 0$ and $K(0) = 0$ and $\boldsymbol{e}_r = \boldsymbol{x}/|\boldsymbol{x}|$ is the radial normal vector. This result is identical to that presented in Refs. [1,3].

Using the same approach for the three-dimensional domain ($d = 3$), we obtain the Green's function:

$$G(\rho) = \frac{1}{2\pi^2\sigma}\frac{\mathrm{Si}(\rho)}{\rho} + C_3 \qquad \text{with} \qquad G(0) = \frac{1}{2\pi^2\sigma} \qquad \text{for} \quad d = 3 \tag{18}$$

Here the integration constant $C_3 = 0$ to impose that $G(\rho) \to 0$ for $\rho \to \infty$ whatever the value of σ.

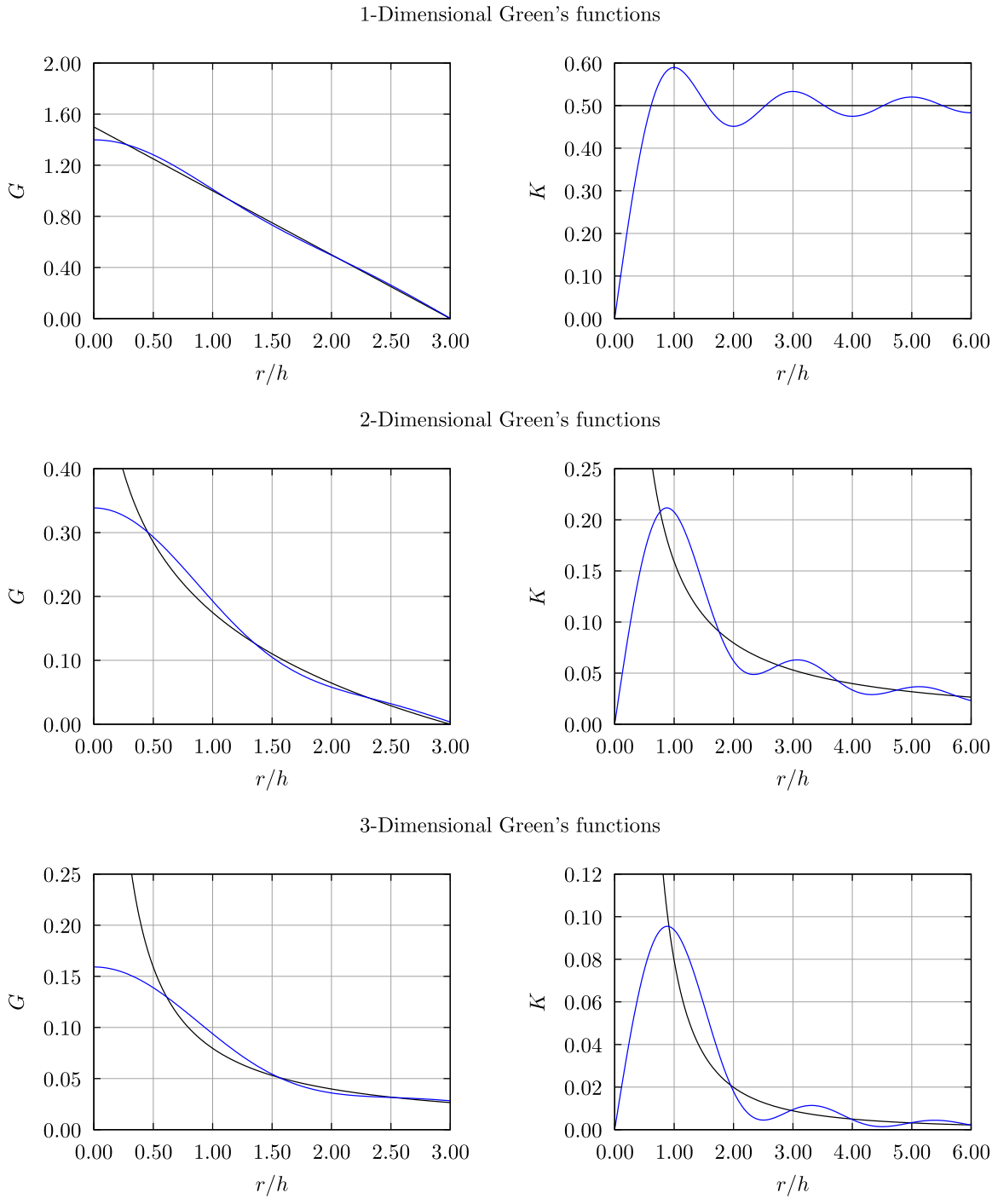

Fig. 1. The regularized Green's functions (blue) compared to the singular Green's functions (black) for the one-, two-, and three-dimensional cases. (Left) The Green's function $G(r)$ (Eqs. (12), (15) and (18)). For the Green's functions in 1D and 2D, $L = 3$ is used to determine the integration constants. (Right) The radial component of the Green's function gradient $K(r)$ (Eqs. (14), (17) and (19)).

The gradient vector of the Green's function is then obtained as:

$$\boldsymbol{K}(\rho) = -K(\rho)\boldsymbol{e}_r \quad \text{with} \quad K(\rho) = -\frac{1}{\sigma}\frac{dG(\rho)}{d\rho} = \frac{1}{2\pi^2\sigma^2}\frac{\mathrm{Si}(\rho) - \sin(\rho)}{\rho^2} \qquad \text{for} \quad d = 3 \tag{19}$$

where we also have that $K(\rho) \geq 0$ and $K(0) = 0$.

The derived non-singular Green's functions are compared to the singular Green's functions in Fig. 1. The oscillatory behavior of the non-singular Green's functions is analogous to the sinc function approximation of the Dirac delta function, and ensures the conservation of the field moments.

For validation we have implemented the non-singular Green's functions into the numerical methodology used in the Poisson solver presented in Refs. [8–10,12]. Using this method we are able to obtain an accuracy in the solution limited only by the machine precision, when tested on the same benchmark cases as is used in [8] (not shown). It is here emphasized that this order of precision is only feasible given a sufficiently smooth and resolved right-hand-side field. For less smooth and resolved fields, the presented non-singular Green's functions still provide the highest possible accuracy allowed by the quadrature error. For the exact numerical implementation that we have used for these tests, the reader is referred to the provided open source software [13].

4. Conclusion

We have derived the non-singular Green's functions for the unbounded Poisson equation, in one, two and in three dimensions, using a spectral regularization method. By applying a radial cut-off function in Fourier space, the regularized Green's function is derived analytically in unbounded domains subject to a minimum resolved length scale (e.g. a mesh size h). As a sharp cut-off function is used, smoothing errors are avoided and the obtained regularized Green's function achieves an optimal accuracy for discretized fields.

The gradient vector of the Green's function was furthermore derived. The obtained Green's function for the two-dimensional case corresponds to that presented in Refs. [1,3]. In the present work, we formally showed the spectral derivation of this function, and we extended it to the one and three-dimensional cases.

Acknowledgment

This research did not receive any specific grant from funding agencies in the public, commercial, or not-for-profit sectors. We would like to acknowledge the helpful support of Henrik Juul Spietz in developing the numerical methodology used in the referenced mesh based Poisson solver.

References

[1] A. Leonard, Vortex methods for flow simulation, J. Comput. Phys. 37 (1980) 289–335.
[2] J.T. Beale, A. Majda, High order accurate vortex methods with explicit velocity kernels, J. Comput. Phys. 58 (1985) 188–208.
[3] G.S. Winckelmans, A. Leonard, Contribution to vortex particle methods for the computation of three-dimensional incompressible unsteady flows, J. Comput. Phys. 109 (1993) 247–273.
[4] F. Vico, L. Greengard, M. Ferrando, Fast convolution with free-space Green's functions, J. Comput. Phys. 323 (2016) 191–203.
[5] J. Carrier, L. Greengard, V. Rokhlin, A fast adaptive multipole algorithm for particle simulations, SIAM J. Sci. Stat. Comput. 9 (4) (1988) 669–686.
[6] J. Barnes, P. Hut, A hierarchical $O(N \log N)$ force-calculation algorithm, Nature 324 (4) (1986) 446–449.
[7] R.W. Hockney, The potential calculation and some applications, Methods Comput. Phys. 9 (1970) 136–210.
[8] M.M. Hejlesen, J.T. Rasmussen, P. Chatelain, J.H. Walther, A high order solver for the unbounded Poisson equation, J. Comput. Phys. 252 (2013) 458–467.
[9] M.M. Hejlesen, J.T. Rasmussen, P. Chatelain, J.H. Walther, High order Poisson solver for unbounded flows, Procedia IUTAM 18 (2015) 56–65.
[10] M.M. Hejlesen, A High Order Regularisation Method for Solving the Poisson Equation and Selected Applications Using Vortex Methods (Ph.D. thesis), Technical University of Denmark, 2016.
[11] P. Chatelain, P. Koumoutsakos, A Fourier-based elliptic solver for vortical flows with periodic and unbounded directions, J. Comput. Phys. 229 (2010) 2425–2431.
[12] H.J. Spietz, M.M. Hejlesen, J.H. Walther, A regularization method for solving the Poisson equation for mixed unbounded-periodic domains, J. Comput. Phys. 356 (2018) 439–447.
[13] M.M. Hejlesen, Open source software available at: https://github.com/mmhej/Poissonsolver.git.

[14] J.T. Rasmussen, Particle Methods in Bluff Body Aerodynamics (Ph.D. thesis), Technical University of Denmark, 2011.
[15] F.W.J. Olver, D.W. Lozier, R.F. Boisvert, C.W. Clark, NIST Handbook of Mathematical Functions, Cambridge University Press, New York, 2010.
[16] Y.L. Luke, Mathematical Functions and their Approximations, Academic Press, Inc., 1975.